Published in final edited form as:
Cardiovasc Res. 2012 April 01; 94(1): 125–135. doi:10.1093/cvr/cvs017.

VEGF-induced endothelial cell migration requires urokinase receptor (uPAR)-dependent integrin redistribution

Revu Ann Alexander[#1], **Gerald W. Prager**[#1,2], **Judit Mihaly-Bison**[1], **Pavel Uhrin**[1], **Stefan Sunzenauer**[3], **Bernd R. Binder**[1,‡], **Gerhard J. Schütz**[3], **Michael Freissmuth**[4], and **Johannes M. Breuss**[1,*]

[1]Institute of Vascular Biology and Thrombosis Research, Vienna A-1090, Austria

[2]Comprehensive Cancer Centre Vienna, Department of Medicine, Medical University of Vienna, Vienna A-1090, Austria

[3]Biophysics Institute, Johannes Kepler University, Linz A-400, Austria

[4]Institute of Pharmacology, Centre of Physiology and Pharmacology, Waehringer Str. 13a, Vienna A-1090, Austria

[#] These authors contributed equally to this work.

Abstract

Aims—Vascular endothelial growth factor (VEGF)-initiated angiogenesis requires coordinated proteolytic degradation of extracellular matrix provided by the urokinase plasminogen activator/urokinase receptor (uPA/uPAR) system and regulation of cell migration provided by integrin–matrix interaction. In this study, we investigated the mechanisms underlying the uPAR-dependent modulation of VEGF-induced endothelial migration.

Methods and results—We used flow cytometry to quantify integrins at the cell surface. Stimulation of human and murine endothelial cells with VEGF resulted in internalization of α5β1-integrins. Micropatterning and immunocytochemistry revealed co-clustering of uPAR and α5β1-integrins and retrieval via clathrin-coated vesicles. It was also contingent on receptors of the low-density lipoprotein receptor (LDL-R) family. VEGF-induced integrin redistribution was inhibited by elimination of uPAR from the endothelial cell surface or by inhibitory peptides that block the uPAR–integrin interaction. Under these conditions, the migratory response of endothelial cells upon VEGF stimulation was impaired both *in vitro* and *in vivo*.

Conclusions—The observations indicate that uPAR is an essential component of the network through which VEGF controls endothelial cell migration. uPAR is a bottleneck through which the VEGF-induced signal must be funnelled for both focused proteolytic activity at the leading edge and for redistribution of integrins.

[*]Corresponding author. Tel: +43 1 4277 62515; fax: +43 1 4277 9625, johannes.breuss@meduniwien.ac.at.
[‡]Deceased on 28 August 2010.

Conflict of interest: none declared.

Europe PMC Funders Author Manuscripts

Keywords

uPAR; Integrin; VEGF; Internalization; Endothelium

1 Introduction

Angiogenesis1 is crucial not only during embryonic development and repair of tissue damage. Tumour cells also recruit endothelial cells to sprout new blood vessels, which support their expansive growth. Vascular endothelial growth factor (VEGF) is the key angiogenic growth factor, because it regulates all steps required for angiogenesis, i.e. induces endothelial cell proliferation and migration, increases vascular permeability, and allows for expression of active proteases on the cell surface.2 As a consequence, matrix molecules are degraded and a new provisional extracellular matrix (ECM) is created that promotes invasion of the surrounding tissue by endothelial cells. The glycosylphosphatidylinositol (GPI)-anchored urokinase receptor (uPAR), a specific receptor for the serine protease urokinase plasminogen activator (uPA), also contributes to ECM remodelling by focusing proteolytic activity on the surface of invading cells.3 In addition, the uPAR system also regulates endothelial cell survival4 and is itself tightly regulated by cell density.5 A link to VEGF-controlled signalling pathways is evident; activation of pro-uPA and uPAR redistributions to focal adhesions are essential steps in VEGF-induced endothelial cell migration *in vitro* and *in vivo*.6,7

Cell migration is contingent on the regulated activation and inactivation of adhesion receptors. Integrins must disengage from ECM contacts at the trailing end and form new focal contacts at the leading edge. This requires continuous and vectorial integrin redistribution. The β1-integrin subfamily is essential for early angiogenesis; a deletion of β1 in vascular endothelial cells is embryonically lethal and causes defects in angiogenic sprouting and vessel branching.8 Integrin ligation with their matrix ligands triggers intracellular signalling via an interaction with molecules that regulate the organization of the actin cytoskeleton. Integrins undergo a transition from a latent form that does not recognize cognate ligands to a binding-competent conformation; uPAR is among the proteins that can impinge on this switch by interacting with integrins of the β2 and of the β1 subfamily.9,10

We have previously shown that the migratory response of endothelial cells to VEGF depends on the uPAR.7 This was observed on vitronectin—an ECM protein which is a ligand for the uPAR.11 This observation suggested that VEGF relied—at least in part—on uPAR to induce endothelial migration. Here, we addressed the question, whether uPAR was necessary for VEGF-induced endothelial migration on fibronectin and other typical ECM components that are not ligands for uPAR. We show that uPAR mediates α5β1-integrin internalization upon VEGF stimulation of endothelial cells. This intracellular sequestration of integrins occurred via clathrin-coated vesicles and was also dependent on low-density lipoprotein receptor (LDL-R) family members. Blocking the association of uPAR and integrins did not only affect integrin redistribution, but also impaired VEGF-stimulated endothelial cell migration *in vitro* and *in vivo*. Thus, in addition to its central role in matrix proteolysis, uPAR is also crucial for integrin redistribution that is necessary to support angiogenesis.

2 Methods

2.1 Materials

The sources of all materials are listed in the Supplementary material online.

2.2 Cell culture

Human umbilical vein endothelial cells (HUVECs) (Technoclone) and murine microvascular endothelial cells were cultured in M199 and Dulbecco modified Eagle medium, respectively, supplemented with 20% foetal calf serum, 22.5 mg/mL heparin, and 3 mg/mL bovine endothelial cell growth supplement. Murine microvascular endothelial cells were isolated from the uterus of uPAR-deficient mice and wild-type littermate controls. Mice were sacrificed by cervical dislocation and pieces of the uteri lacking visible fat tissue were enzymatically treated by a mixture consisting of collagenase A, dispase, and DNase. Subsequently, microvascular endothelial cells were selected using Dynabeads coupled to anti-CD31 antibody and Dynal MPC Magnetic Particle Concentrator (Dynal Biotec). Experiments were performed using quiescent subconfluent cultures up to passage 5. Cells were rendered quiescent by serum withdrawal (24 h 5% FCS, 4 h serum-free M199 containing 1% BSA).

2.3 Flow cytofluorometry

Subconfluent endothelial cells were treated as indicated with growth factors ($VEGF_{165}$, VEGF-E) for the appropriate time. Following stimulation, the cells were washed with ice-cold PBS, harvested with 3 mM EDTA, and fixed with 4% paraformaldehyde for 15 min. In some instances, a parallel culture was permeabilized with 0.2% Triton X-100 for 10 min. After blocking with 2% goat serum, the appropriate primary antibody was added for 60 min at room temperature. Following a PBS wash, the samples were incubated with the appropriate Alexa Fluor 488-conjugated secondary antibody, washed and analysed with FACSort (Becton-Dickinson). In the case of experiments using inhibitors or peptides, the cells were pre-treated with the appropriate amounts for 10 min prior to stimulation. For the siRNA experiments, HUVECs were transfected with uPAR siRNA (100 nM) using X-tremeGENE siRNA transfection reagent according the manufacturer's instructions. After 36 h, cells were stimulated with VEGF and analysed as earlier.

2.4 Surface biotinylation and immunoblotting

HUVECs were washed with ice-cold PBS (pH 8.0) and incubated with 2 mM sulfo-NHS-LC-biotin for 30 min on ice, either before or after VEGF stimulation. Following a wash in ice-cold glycine (200 mM, in PBS, pH 7.0) to remove excess biotin, the samples were lysed in a RIPA buffer for 30 min on ice. The biotinylated surface proteins were adsorbed by overnight incubation with streptavidin-coated Sepharose 4B beads. The beads were washed three times with the RIPA buffer and the adsorbed material eluted by boiling in non-reducing sample buffer. Proteins were separated on SDS polyacrylamide gels, transferred to PVDF membrane and probed with relevant antibodies. Immunoreactive bands were detected by enhanced chemiluminescence.

2.5 Immunocytochemistry

The samples were fixed with 4% paraformaldehyde for 15 min, permeabilized with 0.1% Triton X-100 for 5 min, and blocked with 5% goat serum for 1 h at room temperature. Samples were stained with the specific primary antibodies for 2 h at 37°C. After washing and incubation with the appropriate secondary antibodies for 2 h at 37°C, samples were mounted in Vectashield and visualized on an Olympus AX70 microscope or a Zeiss LSM510.

2.6 Micropatterning

The micropatterning experiment was performed as previously described12 with the following modifications. Polydimethylsiloxane stamps containing the microarray were generated by the standard photolithography. Stamps were rinsed with 100% ethanol and water, dried under N_2, and incubated with 100 mg/mL Cy5-labelled BSA for 30 min at room temperature. The stamps were washed and dried as before and placed under their own weight onto epoxy-derivatized glass coverslips for 1 h. Upon removing the stamps, the coverslips were sealed with adhesive silicone masks. The glass coverslips that were coated with a Cy5-labelled BSA micropattern were then incubated with 50 µg/mL of streptavidin and incubated with 10 µg/mL biotinylated monoclonal antibody. Endothelial cells were seeded on micropatterns and allowed to adhere. Following stimulation, samples were fixed with 4% paraformaldehyde. They were stained for uPAR with the monoclonal mouse 3937 antibody (pre-labelled with Alexa Fluor 488-conjugated Fab fragments) for 60 min. Images were acquired on a Axiovert 200/M microscope (Zeiss) in the total internal reflection configuration using oil immersion (objective magnification = 100-fold). Images were analysed using a semi-automated image and data analysis software that was developed in-house; an automatic gridding algorithm calculates the grid size and the rotation angle φ of the image. The grid subdivides the total image into adjacent squares, which are quantified according to the average specific signal with a central circle (F^+) and unspecific background outside the circle (F^-). This information is used to calculate fluorescence (F) and contrast (C).

2.7 Migration assay

For the Transwell™ migration assay, serum-starved HUVECs (25 000) treated with or without the inhibitory peptides (25 µM) were seeded on 8 µm pore Transwell™ inserts coated with 5 µg/mL fibronectin. After 4 h, the cells that had not migrated were removed from the upper chamber. Migrated cells were fixed with 4% paraformaldehyde, stained with Hoechst (DAPI) 1:1000 for 15 min and counted using a 10× objective of an Olympus AX70 microscope.

2.8 *In vivo* angiogenesis

A subcutaneously deposited matrigel plug was used to assess angiogenesis *in vivo* as previously described.7 Briefly, mice were anaesthetized with ketamin (100 mg/kg) and xylazin (10 mg/kg); when mice did not react to pinching, growth factor-depleted matrigel solution (0.3 mL) supplemented with vehicle or 300 ng/mL $VEGF_{164}$ with and without 200 nM receptor-associated protein (RAP) was subcutaneously injected into their flanks. Eight-

to 14-week-old uPAR-deficient ($n = 7$) and wild-type littermate control males ($n = 7$) were used. The mice were sacrificed on the eighth day by cervical dislocation. The matrigel plugs were removed and frozen in liquid N_2. Sections of the frozen plugs were stained with haematoxylin, DAPI or rat anti-mouse CD31 antibody. Tissue samples were visualized with an AX-70 Olympus microscope and photographed using an Optronics DEI-750D CCD camera. The directed *in vivo* angiogenesis assay (DIVAA) was performed according to the manufacturers' instructions (Supplementary material online, Methods). The experiments were approved by the Animal Welfare Committee of the Medical University of Vienna and the Austrian Ministry of Science and Research (License No. 66.009/0178-BrGT/2006 and 66.009/0103-C/GT/2007). The investigation conforms with the *Guide for the Care and Use of Laboratory Animals* published by the Directive 2010/63/EU of the European Parliament.

2.9 Statistics

Statistical significance was assessed by using Student's *t*-test for paired observations. Multiple comparisons were done by ANOVA and Dunnett's *post hoc* test.

3 Results

3.1 VEGF induces internalization of β_1-integrins

In VEGF-induced sprouting of capillaries, endothelial cells must reorganize their contacts with the ECM. We focused on the β1 subfamily of integrins, because members of this subfamily are considered to be the adhesion molecules utilized in the unstimulated, resting state of endothelial cells.13 $VEGF_{165}$ stimulation of quiescent endothelial cells resulted in a marked redistribution of β1-integrins. In resting endothelial cells, the β1-integrin subunit was found mainly at the cell periphery: the immunoreactivity outlined the cell borders (Figure 1A, control). In contrast, in $VEGF_{165}$-stimulated endothelial cells immunostaining at the cell borders declined and increased in the vicinity of the nuclei (Figure 1A, VEGF). This shift suggested that VEGF caused internalization of integrins. We confirmed this internalization by assessing the amount of β1-integrins at the cell surface before and after VEGF stimulation on non-permeabilized cells. In parallel, permeabilized cells were assessed for changes in the total cellular amount of the β1-integrin subunit. As shown in Figure 1B and Supplementary material online, Figure S1, $VEGF_{165}$ stimulation of endothelial cells resulted in an ~30% decrease in the amount of β1-integrins at the cell surface (non-permeabilized cells, red histograms). VEGF did not affect the total amount of β1-integrins (permeabilized cells, black histograms). In addition, we confirmed the internalization of β1-integrins by cell surface biotinylation of endothelial cells (Figure 1C). If cell surface proteins were biotinylated prior to $VEGF_{165}$ stimulation, the amount of biotinylated β1-integrins recovered from the whole cell lysates did not differ between stimulated and unstimulated cells (Figure 1C, right-hand lanes). However, if cells were subjected to biotinylation after they had been exposed to VEGF, we observed a decline (by 30–40%) of biotinylated β1-integrins when compared with unstimulated cells. Thus, both approaches provided incontrovertible evidence for VEGF-induced internalization of β1-integrins in endothelial cells.

3.2 uPAR and β1-integrins interact and co-internalize upon VEGF stimulation

We previously observed that, within a similar time interval, VEGF also caused internalization of the uPAR.8 We therefore explored if uPAR and β1-integrins co-clustered and co-internalized upon VEGF stimulation. This was the case: in unstimulated endothelial cells, β1-integrins were mainly found at the cellular periphery, β3-integrins in the perinuclear compartment, and uPAR was distributed in a distinct but diffuse pattern (Figure 2A, control). Treatment with $VEGF_{165}$ led to the redistribution of uPAR to the newly formed focal adhesions, where it co-localized with β3-integrins. Finally, treatment with VEGF reduced co-locolization of integrin subunit β1 with pFAK but augmented that with uPAR in vesicular structures (Supplementary material online, Figure S3). These observations confirmed co-internalization of β1-integrins and uPAR into the same endocytotic vesicles (Figure 2A, VEGF). The addition of VEGF also induced co-localization of uPAR and β1 integrins in polarized cells, which had migrated into the cell-free area created by scratching the endothelial monolayer, (Supplementary material online, Figure S6). Integrin and uPAR redistribution was not observed, if endothelial cells were incubated with RAP prior to stimulation with VEGF (Figure 2A, VEGF/RAP). RAP precludes complex formation between uPAR and LDL-R family-like proteins and their internalization.8,14 This indicated that an LDL-R-like protein mediated the co-internalization of uPAR and β1-integrins.

We used micropatterning as an independent approach to demonstrate the interaction between uPAR and integrins in VEGF-stimulated endothelial cells. The micropatterning technique was recently introduced as a method to assess protein–protein interactions on the surface of living cells.12 It relies on the immobilization of a given antibody in a geometric pattern on a glass coverslip. We used an antibody to the β1-integrin subunit. Accordingly, on attaching and spreading cells β1-integrins were captured at these spots of immobilized antibody (not shown). In unstimulated cells, uPAR was distributed homogeneously with occasional punctuate staining (Figure 2Ba). In contrast, upon VEGF stimulation of endothelial cells uPAR was redistributed to the pattern defined by the immobilized integrin antibody (Figure 2Bc). The quantitative analysis for the single spot fluorescence yielded a mean contrast of 0.35 (Figure 2Bd) for stimulated cells and a mean contrast of 0.07 for unstimulated cells (Figure 3Bb). This high mean contrast between areas of antibody spots and the background BSA grid provides a quantitative readout and documents that VEGF caused uPAR to become enriched in areas of immobilized integrins. In contrast, if an activating antibody against integrin subunit β1 was used as bait, we did not observe any association between uPAR and β1-integrins upon VEGF stimulation (Figure 2C). These observations and earlier findings6 are consistent with the notion that integrins need to be in their inactive state to allow for VEGF-induced complex formation with uPAR.

Stimulation of VEGFR-2 triggers several signalling pathways [e.g. phospholipase C-γ-mediated protein kinase C activation, RAS-dependent ERK activation, stimulation of Src kinase (SRC), etc]. We recently observed that activation of a receptor tyrosine kinase and of LRP-1 in the presence of uPAR resulted in sustained ERK activation and increased cellular adhesion.15 VEGF-induced uPAR internalization via a signalling pathway comprising VEGFR-2, PI3-kinase and matrix metalloproteinase (MMP-2).6 Accordingly, we interrogated the signalling network underlying integrin internalization by using several

inhibitors, i.e. the PI3-kinase inhibitor wortmannin, the MMP-2/9 inhibitor (2*R*)-2-[(4-biphenylylsulfonyl)amino]-3-phenylpropionic acid, the MEK1-inhibitor PD98050 (to block activation of ERK1/2), the inhibitor of PLC-γ U73122 and PP1 to suppress the non-receptor tyrosine kinase SRC. Serum-starved endothelial cells were pre-treated with these inhibitors and stimulated with VEGF-E, the specific ligand for VEGFR-2 and with PlGF, the specific ligand for VEGFR-1. Flow cytometry showed that VEGF-E-induced but not PlGF-induced internalization of β1-integrins was blunted upon inhibition of PI3-kinase and MMP-2/9 inhibitor (Figure 2D). In contrast, neither VEGF-E- nor PlGF-stimulated internalization of uPAR or integrins was inhibited by inhibition of ERK1/2, SRC, or PLC (not shown). Taken together, our results show that internalization of β1-integrins is controlled by the same pathway (i.e. VEGFR-2 and PI3-kinase-dependent activation of MMP-2) as recycling of uPAR.

3.3 The presence of uPAR is essential for VEGF-induced internalization of β1-integrins into clathrin-coated vesicles

The uPAR is internalized in a trimeric uPAR/uPA/PAI-1 complex via clathrin-coated vesicles in response to addition of the uPA:PAI-1 complex.14 If uPAR and β1-integrins are co-internalized, β1-integrins must also be found in clathrin-coated vesicles. Upon $VEGF_{165}$ stimulation of HUVECs, β1-integrins co-localized with the clathrin heavy chain (Figure 3A, VEGF) in vesicle-like structures. The clathrin-mediated internalization of integrins and the concomitant internalization of uPAR may happen by co-incidence. Alternatively, complex formation may be required to drive efficient endocytosis of integrins. We employed two different approaches to discriminate between these two possibilities. In the first approach, endothelial cells were pre-treated with phosphatidylinositol-specific phospholipase C (PI-PLC) to cleave off all GPI-anchored proteins including uPAR from the cell surface. They were then stimulated with VEGF-E; surface integrin levels were subsequently assessed by flow cytofluorometry. The lack of uPAR impaired VEGF-induced internalization of β1-integrins (Figure 3B).

Our second approach relied on confocal microscopy. Murine endothelial cells lacking the uPAR were analysed for their ability to redistribute integrins to clathrin-coated structures upon stimulation with $mVEGF_{164}$. In wild-type mouse endothelial cells $mVEGF_{164}$ induced a significant, albeit small (~20%) increase in the co-localization of β1-integrins and clathrin (Figure 3C). As expected, this increase in co-localization was inhibited by pre-treatment with RAP. In $uPAR^{-/-}$ murine endothelial cells, no increase in the co-localization of clathrin and β1-integrins was detectable upon $mVEGF_{164}$ stimulation. Similarly, pre-treatment with RAP before $mVEGF_{164}$ stimulation did not cause any change in the extent of co-localization. These data indicate that VEGF-induced integrin internalization is dependent on the presence and co-internalization with uPAR to reach clathrin-coated vesicles.

3.4 Integrin-α5β1 associates with uPAR for VEGF-induced endocytosis

At least six different β1-integrin heterodimers have been identified on endothelial cells.13 We analysed the VEGF-induced change in surface localization of these different α-integrin subunits (not shown). These experiments revealed that α3β1- and α5β1-integrins were internalized upon $VEGF_{165}$ stimulation. We examined whether α5β1 or α3β1 interact with

uPAR upon VEGF stimulation by employing the micropatterning approach. Micro-biochip surfaces were functionalized with an antibody to either integrin subunit. This forced the α3β1- or α5β1-integrins on adhering cells to accumulate according to the pattern of the immobilized antibody. In the case of VEGF-stimulated cells, uPAR accumulated in the spots of immobilized integrin α5β1 (Figure 4Ab). This can only be accounted for by a VEGF-induced interaction between uPAR and α5β1. The patterned antibody to integrin α5β1 did not cause any patterning of uPAR upon VEGF stimulation, indicating no appreciable interaction (Figure 4Bb).

Different amino acid residues in domain-3 have been implicated in the interaction of uPAR with β1-integrins. We synthesized peptide 243–251 which contains two implicated residues S245 and H24916,17 to define the region within uPAR that provides the necessary interaction needed for integrin internalization. We assessed whether the internalization of α5β1 was dependent on uPAR by using this inhibitory peptide. Analysis of surface expression of α5β1 and α3β1 by FACS shows that addition of $VEGF_{165}$ led to internalization of ~25 and ~35% of integrin α3β1 and α5β1, respectively. Pre-treatment with the peptide inhibited the VEGF-induced internalization of α5β1 (Figure 5A, for the concentration–response curve, see Supplementary material online, Figure S5) but not that of α3β1 (Figure 5B). In contrast, the scrambled peptide did not have any inhibitory effect (Figure 5A and B). The peptides did not affect the VEGF-induced internalization of uPAR (Figure 5C) indicating that the requirements for co-internalization were asymmetrical; internalization of integrin α5β1 was contingent on complex formation with uPAR, but VEGF-driven endocytosis of uPAR did not require an interaction with integrin-α5β1. As an additional proof of concept, knock-down of uPAR by siRNA also blocked VEGF-induced internalization of the fibronectin receptor α5β1, (Figure 5D and Supplementary material online, Figure S5). RAP is known to inhibit VEGF-induced internalization of uPAR.7 Thus, RAP is predicted to inhibit the internalization of both, uPAR and integrin-α5β1, if the complex assembles in a hierarchical order. Pre-treatment of endothelial cells with RAP indeed inhibited the internalization of α5β1 (Figure 5E). As expected, this was not the case for α3β1 (Figure 5F). Taken together, these data are consistent with the VEGF-driven assembly of a complex comprising integrin-α5β1, uPAR, and an LDLR-like protein that is required for the internalization of α5β1.

3.5 VEGF-induced endothelial cell migration requires internalization of the uPAR–integrin complex

Integrin-α5β1 is a fibronectin receptor and fibronectin is an essential component of the provisional ECM generated during wound healing and angiogenesis,13 but it is not a ligand for the uPAR. However, in our model blockage of uPAR recycling is predicted to impair migration because efficient integrin recycling is contingent on the co-internalization of uPAR, integrins, and LDLR-like protein. We therefore examined whether the uPAR inhibitory peptide (which precluded uPAR–integrin interaction) and RAP (which precluded LDLR-like protein-mediated uPAR-integrin internalization) suppressed VEGF-induced migration of endothelial cells on fibronectin. This was the case. In a modified Boyden chamber chemotaxis assay, the inhibitory peptide (Figure 6A) and RAP (Figure 6B)

significantly reduced migration towards VEGF. In contrast, the scrambled peptide did not have any appreciable effect (Figure 6A).

This also predicts that inhibition of uPAR-mediated integrin recycling must have an effect on endothelial cell migration *in vivo*. This prediction was verified by subcutaneous injection of control matrigel suspensions or of matrigel containing $mVEGF_{164}$ or the combination of $mVEGF_{164}$ and RAP. VEGF provides the chemo-attractant stimulus for endothelial cells, which invade the matrigel, deposit additional ECM including fibronectin, and form blood vessels. We compared endothelial invasion into an $mVEGF_{164}$-containing matrigel plug in wild-type mice (Figure 6C, top) and $uPAR^{-/-}$ (Figure 6C, bottom). Consistent with previous results,7 the presence of $mVEGF_{164}$ promoted the invasion of the matrigel plug and the appearance of vessel-like structures within the matrigel (Figure 6Cb). This was suppressed by the concomitant presence of RAP in the matrigel plug (Figure 6Cc). In $uPAR^{-/-}$ mice, $mVEGF_{164}$ had only a very modest effect on cell invasion (Figure 6Ce) and this was not affected by RAP (Figure 6Cf).

We used a second approach to inhibit uPAR-mediated integrin recycling and thus endothelial migration and angiogenesis *in vivo*; we investigated the anti-angiogenic effect of the uPAR-derived peptide m.P243-251 in a DIVAA. The peptide m.P243-251 ‘TASWCQGSH’ corresponds to the domain-3 peptide of human uPAR (Figure 5A). Angioreactors filled with basement membrane extract containing either mVEGF or the combination of mVEGF and m.P243-251 were subcutaneously implanted for 11 days in the dorsal flanks of wild-type mice. As predicted, capillary tubes formed in reactors containing mVEGF. In contrast, angiogenesis was significantly inhibited in reactors filled with VEGF and the inhibitory peptide m.P243-251 (Figure 6Da). The presence of endothelial cells was verified by immunostaining sections from the reactors for CD31 (Figure 6Db and c). These observations are consistent with the interpretation that uPAR-mediated integrin internalization is a necessary step in VEGF-induced cell migration and invasion.

4 Discussion

VEGF-directed reprogramming shifts endothelial cells from quiescence to an activated state that enables invasion of the surrounding tissue. Invasion is supported by the redistribution of uPAR to the leading edge of endothelial cells, which results in focused proteolysis of the ECM.7 This is achieved by complex formation between the GPI-anchored uPAR and a member of the LDL-receptor family and the subsequent internalization of the complex.14 VEGF drives this endosomal recycling of uPAR by a signalling cascade that emanates from the VEGF-receptor-2/Flk1.7 Our current observations document that the VEGF signal is funnelled through uPAR to control a second, integrin-dependent limb of the angiogenic response. VEGF-induced recycling of the integrin α5β1 uPAR and is contingent on the clathrin-dependent internalization of a complex that contains an LDLR-like protein. This conclusion is based on the following findings: (i) VEGF promoted assembly of a complex comprising integrin α5β1. (ii) The internalization of the complex into the same intracellular compartment, namely endosomes that were also decorated with clathrin immunoreactivity was mediated by LDLR-like protein. (iii) In the absence of uPAR, VEGF failed to trigger internalization of integrin α5β1 and thus initiate the redistributive cycle of integrin

endocytosis and exocytosis. This translated into impaired endothelial cell migration *in vitro* and reduced endothelial cell invasion and vessel formation *in vivo*.

Earlier experiments suggested a functional interaction of integrin α5β1 and uPAR: upon increasing expression of uPAR, integrin α5β1 was recovered in the immunoprecipitate and this correlated with persistent ERK1/2 activation and enhanced tumour growth *in vivo*.18 We employed a micropatterning approach that allowed for direct visualization of VEGF-promoted formation of a complex between uPAR and integrin α5β1 on the endothelial cell surface. The fact that integrin internalization is precluded in this experimental set-up did not only facilitate quantitative assessment of uPAR recruitment but also afforded the unequivocal demonstration that the interaction happened indeed at the cell surface. This new approach does not differentiate whether there is a direct interaction between uPAR and integrins or whether additional proteins—other than LDLR-like proteins—must be recruited to stabilize and internalize the complex. In fact, purified uPAR and purified integrin α5β1 can directly interact in detergent solution.16 However, our observations show that in the cell membrane the interaction is subject to regulation. VEGF may either promote a conformational change that increases the mutual affinity of the partners or drive the association by recruiting an additional molecule into the complex. This is underscored by the fact that the activating antibody to integrin α5β119 inhibited the VEGF-induced recruitment of uPAR in the micropatterning experiment.

In endothelial cells, VEGF triggered endocytosis of integrin α3β1. Previous experiments documented that the binding of integrin α3β1 to uPAR occurred in a uPA-dependent manner.20 The direct binding of purified uPAR to purified integrin α3β1 and the recovery of uPAR in complex with integrin-α3β1 is contingent on the presence of uPA.20,21 Surprisingly, micropatterning did not detect any direct interaction of integrin α3β1 with uPAR. In our opinion, micropatterning is among the most sensitive methods to record interactions in the native cell membrane, because it does not require any modification of the interacting molecules (e.g. by attaching fluorescent moieties) or any change in their stoichiometry (e.g. by heterologous expression). Thus, we conclude that, in endothelial cells, VEGF does not promote complex formation between integrin-α3β1 and uPAR. This conclusion is also supported by the observation that VEGF-triggered endocytosis of integrin α3β1 was not impaired by RAP. The discrepancy between our findings and results from earlier studies20,21 is most likely accounted for by cell type-dependent differences. In fact, uPAR can recruit various integrins9,16,20 in a cell type-dependent manner. This also supports the conjecture that these complexes are stabilized by the recruitment of additional proteins.

Our observations support a model, where the VEGF-induced signal is propagated via uPAR to reduce integrin α3β1-mediated endothelial adhesion. While the VEGF-induced surface localization of integrin-αvβ3 is predicted to enhance adhesion, the increase in the turnover of α5β1 reduces adhesion and fosters endothelial cell migration. This predicts that the absence of integrin-α5β1 ought to suppress tumour angiogenesis. In fact, blockage of integrin α5β1 by an antibody suppressed angiogenesis in a murine tumour model, where human rhabdomyosarcoma cells were xenografted into immunodeficient mice.22 Accordingly, integrin-α5β1 is being explored as a potential target in advanced human

cancer; the pertinent chimeric antibody, is currently in phase II clinical trials.23 The binding sites for integrin-α5β1 are thought to reside on domain-3 of uPAR. Specifically, point mutation of S245 or H249 resulted in inhibition of the association of uPAR and integrin-α5β1.16,17 This allows for selective disruption of the complex, a concept that was verified by using a peptide comprising the residues 243–251 of uPAR (TASMCQHAH) that contains both S245 and H249. The peptide efficiently blocked VEGF-induced internalization of the fibronectin receptor *in vitro* and angiogenesis *in vivo*. The interaction site between uPAR and integrin α5β1 fulfils several criteria of a candidate drug binding site: (i) it is readily accessible, because it is on the extracellular surface, thus obviating the cell membrane as a permeation barrier. (ii) It allows for discrimination because it can be specifically targeted. (iii) There is no major toxicity that can be *a priori* anticipated. The absence of uPAR allows for the development of a viable animal24 but it interferes with VEGF-induced angiogenesis. Our results therefore provide a proof-of-principle that the interface of uPAR and integrin α5β1 may represent a site to be targeted for anti-angiogenic therapy.

Supplementary Material

Refer to Web version on PubMed Central for supplementary material.

Acknowledgements

We thank Gunilla Hoyer-Hansen for kindly providing the uPAR monoclonal antibody R2.

Funding

This work was supported in part by grants from the Austrian Science Foundation/FWF (FWF P21301 to G.W.P. and B.R.B), EU 6th Framework Integrated Project Cancer Degradome (LSHC-CT-2003-503297), International-PhD program ‘Cell Communication in Health and Disease’ sponsored by the Austrian Science Fund/FWF and the Medical University of Vienna, and by the Österreichische Nationalbank Jubiläumsfondprojekt 13204 to J.M.B. S.S. is a recipient of a DOC fellowship of the Austrian Academy of Sciences, Institute of Biophysics, Linz.

References

1. Folkman J. Proceedings: tumor angiogenesis factor. Cancer Res. 1974; 34:2109–2113. [PubMed: 4842257]
2. Carmeliet P. Angiogenesis in health and disease. Nat Med. 2003; 9:653–660. [PubMed: 12778163]
3. Koolwijk P, Sidenius N, Peters E, Sier CF, Hanemaaijer R, Blasi F, et al. Proteolysis of the urokinase-type plasminogen activator receptor by metalloproteinase-12: implication for angiogenesis in fibrin matrices. Blood. 2001; 97:3123–3131. [PubMed: 11342439]
4. Prager GW, Mihaly J, Brunner PM, Koshelnick Y, Hoyer-Hansen G, Binder BR. Urokinase mediates endothelial cell survival via induction of the X-linked inhibitor of apoptosis protein. Blood. 2009; 113:1383–1390. [PubMed: 18948573]
5. Brunner PM, Heier PC, Mihaly-Bison J, Priglinger U, Binder BR, Prager GW. Density enhanced phosphatase-1 down-regulates urokinase receptor surface expression in confluent endothelial cells. Blood. 2011; 117:4154–4161. [PubMed: 21304107]
6. Prager GW, Breuss JM, Steurer S, Mihaly J, Binder BR. Vascular endothelial growth factor (VEGF) induces rapid prourokinase (pro-uPA) activation on the surface of endothelial cells. Blood. 2004; 103:955–962. [PubMed: 14525763]
7. Prager GW, Breuss JM, Steurer S, Olcaydu D, Mihaly J, Brunner PM, et al. Vascular endothelial growth factor receptor-2-induced initial endothelial cell migration depends on the presence of the urokinase receptor. Circ Res. 2004; 94:1562–1570. [PubMed: 15131009]

Europe PMC Funders Author Manuscripts

8. Tanjore H, Zeisberg EM, Gerami-Naini B, Kalluri R. Beta1 integrin expression on endothelial cells is required for angiogenesis but not for vasculogenesis. Dev Dyn. 2008; 237:75–82. [PubMed: 18058911]
9. Bohuslav J, Horejsi V, Hansmann C, Stöckl J, Weidle UH, Majdic O, et al. Urokinase plasminogen activator receptor, β2-integrins, and Src-kinases within a single receptor complex of human monocytes. J Exp Med. 1995; 181:1381–1390. [PubMed: 7535337]
10. Wei Y, Lukashev M, Simon DI, Bodary SC, Rosenberg S, Doyle MV, et al. Regulation of integrin function by the urokinase receptor. Science. 1996; 273:1551–1555. [PubMed: 8703217]
11. Wei Y, Waltz DA, Rao N, Drummond RJ, Rosenberg S, Chapman HA. Identification of the urokinase receptor as an adhesion receptor for vitronectin. J Biol Chem. 1994; 269:32380–32388. [PubMed: 7528215]
12. Schwarzenbacher M, Kaltenbrunner M, Brameshuber M, Hesch C, Paster W, Weghuber J, et al. Micropatterning for quantitative analysis of protein-protein interactions in living cells. Nat Methods. 2008; 5:1053–1060. [PubMed: 18997782]
13. Mettouchi A, Meneguzzi G. Distinct roles of beta1 integrins during angiogenesis. Eur J Cell Biol. 2006; 85:243–247. [PubMed: 16546568]
14. Czekay RP, Kuemmel TA, Orlando RA, Farquhar MG. Direct binding of occupied urokinase receptor (uPAR) to LDL receptor-related protein is required for endocytosis of uPAR and regulation of cell surface urokinase activity. Mol Biol Cell. 2001; 12:1467–1479. [PubMed: 11359936]
15. Geetha N, Mihaly J, Stockenhuber A, Blasi F, Uhrin P, Binder BR, et al. Signal integration and coincidence detection in the mitogen-activated protein kinase/extracellular signal-regulated kinase (ERK) cascade: concomitant activation of receptor tyrosine kinases and of LRP-1 leads to sustained ERK phosphorylation via down-regulation of dual specificity phosphatases (DUSP1 AND -6). J Biol Chem. 2011; 286:25663–25674. [PubMed: 21610072]
16. Chaurasia P, Aguirre-Ghiso JA, Liang OD, Gardsvoll H, Ploug M, Ossowski L. A region in urokinase plasminogen receptor domain III controlling a functional association with alpha5beta1 integrin and tumor growth. J Biol Chem. 2006; 281:14852–14863. [PubMed: 16547007]
17. Wei Y, Tang CH, Kim Y, Robillard L, Zhang F, Kugler MC, et al. Urokinase receptors are required for α5β1 integrin-mediated signaling in tumor cells. J Biol Chem. 2007; 282:3929–3939. [PubMed: 17145753]
18. Aguirre Ghiso JA, Kovalski K, Ossowski L. Tumor dormancy induced by downregulation of urokinase receptor in human carcinoma involves integrin and MAPK signaling. J Cell Biol. 1999; 147:89–104. [PubMed: 10508858]
19. Mould AP, Garratt AN, Askari JA, Akiyama SK, Humphries MJ. Identification of a novel anti-integrin monoclonal antibody that recognises a ligand-induced binding site epitope on the beta 1 subunit. FEBS Lett. 1995; 363:118–122. [PubMed: 7537221]
20. Mazzieri R, D'Alessio S, Kenmoe RK, Ossowski L, Blasi F. An uncleavable uPAR mutant allows dissection of signaling pathways in uPA-dependent cell migration. Mol Biol Cell. 2006; 17:367–378. [PubMed: 16267271]
21. Wei Y, Eble JA, Wang Z, Kreidberg JA, Chapman HA. Urokinase receptors promote beta1 integrin function through interactions with integrin alpha3beta1. Mol Biol Cell. 2001; 12:2975–2986. [PubMed: 11598185]
22. Bhaskar V, Zhang D, Fox M, Seto P, Wong MH, Wales PE, et al. A function blocking anti-mouse integrin alpha5beta1 antibody inhibits angiogenesis and impedes tumor growth in vivo. J Transl Med. 2007; 5:61. [PubMed: 18042290]
23. Bell-McGuinn KM, Matthews CM, Ho SN, Barve M, Gilbert L, Penson RT, et al. A phase II, single-arm study of the anti-α5β1 integrin antibody volociximab as monotherapy in patients with platinum-resistant advanced epithelial ovarian or primary peritoneal cancer. Gynecol Oncol. 2011; 121:273–279. [PubMed: 21276608]
24. Dewerchin M, Nuffelen AV, Wallays G, Bouche A, Moons L, Carmeliet P, et al. Generation and characterization of urokinase receptor-deficient mice. J Clin Invest. 1996; 97:870–878. [PubMed: 8609247]

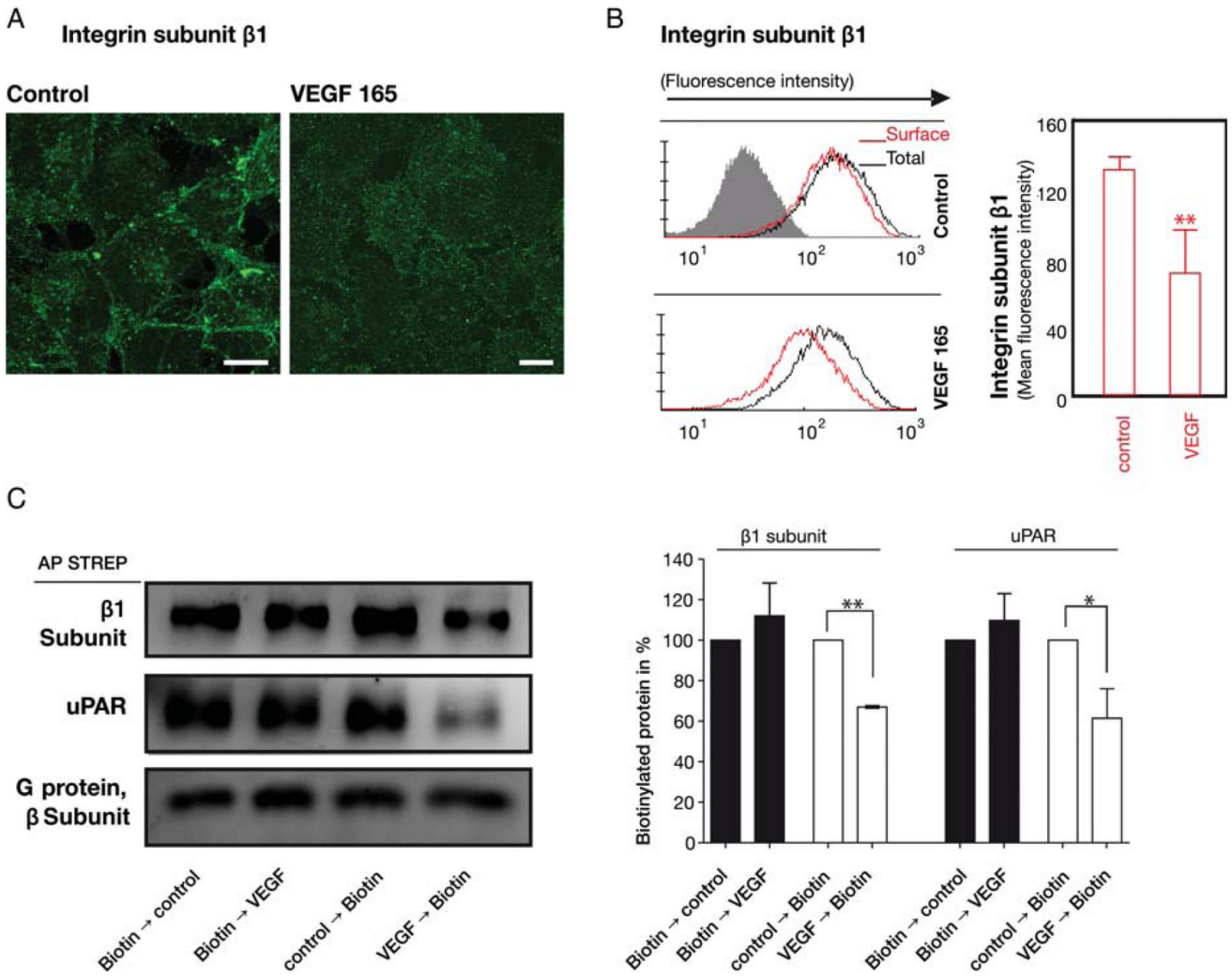

Figure 1.

VEGF-induced internalization of β1-integrins in endothelial cells. (*A*) $VEGF_{165}$ stimulated redistribution of β1-integrins visualized by confocal microscopy: the integrin subunit β1 (green) was detected by indirect immunofluorescence in fixed, permeabilized human umbilical vein endothelial cells (HUVECs); scale bars 10 μm. (*B*) Internalization of β1-integrins was determined by flow cytofluorimetry of non-permeabilized (cell surface β1, red histogram) and permeabilized (total cellular β1 amount, black histogram) HUVECs incubated in the absence and presence of $VEGF_{165}$ (50 ng/mL) for 15 min. The bar diagram summarizes the quantitative analysis (mean ± standard deviation) of cell surface β1-integrins calculated from the geometric mean fluorescence values ($n = 3$). (*C*) Cell surface proteins were biotinylated either before or after $VEGF_{165}$ stimulation for 60 min and enriched by affinity precipitation on streptavidin beads from detergent extracts; biotinylated uPAR and β1-integrins was detected by immunoblotting and quantified by densitometry relative to the unstimulated control, which was the 100% reference value. Immunoblotting with an antiserum recognizing all G protein β-subunits was done as a loading control. Mean ± standard deviation ($n = 3$), $^{**}P < 0.01$, *t*-test for paired data.

Europe PMC Funders Author Manuscripts

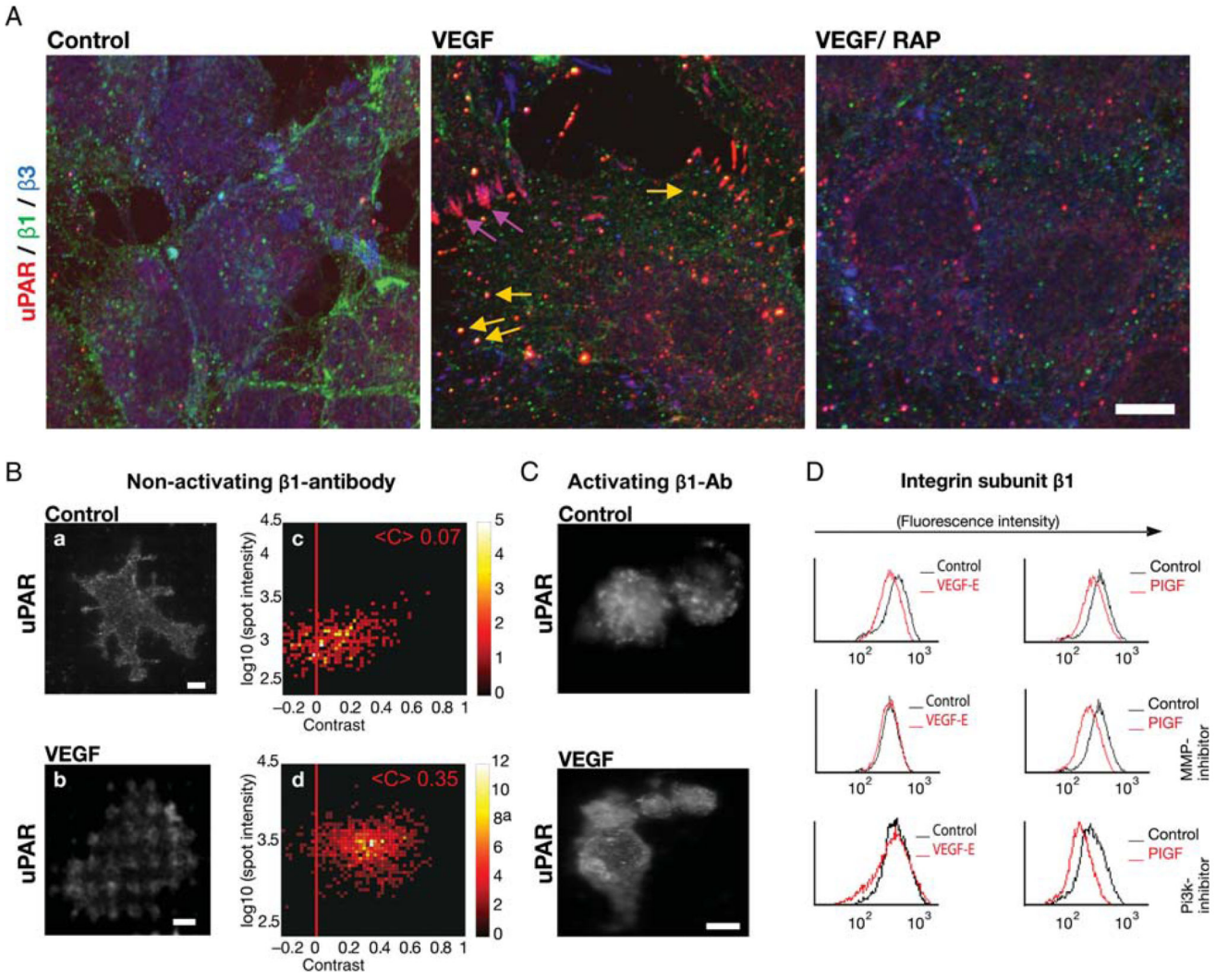

Figure 2.

VEGF-induced co-internalization of β1-integrins and uPAR. (*A*) Co-localization of uPAR with β1-integrins and with integrin-αvβ3 in intracellular vesicles and in focal adhesions, respectively, of $VEGF_{165}$-stimulated HUVECs that were fixed and subjected to triple immunofluorescence staining for β3-integrins (green), uPAR (red), and β1-integrins (blue). Scale bar 10 μm. (*B*) Cell surface interaction between uPAR and β1-integrins assessed by micropatterning. Endothelial cells were grown on functionalized glass coverslips, with grids of BSA-Cy5 printed on them and interspaces coated with streptavidin and biotinylated non-activating monoclonal antibody against integrin subunit β1. After stimulation with $VEGF_{165}$ (50 ng/mL) for 60 min, samples were fixed and immunostained with a pre-labelled uPAR monoclonal antibody. The VEGF-induced redistribution of uPAR was visualized by TIRF-microscopy. Scale bar 6 μm. Statistical analysis for the single spot fluorescence brightness F and contrast C of multiple cells ($n = 64$) is represented in a colour density plot with the mean contrast indicated. (*C*) HUVECs were grown and treated as in (*B*) on a surface patterned by immobilizing an activating antibody against β1-integrins, which precluded any appreciable

VEGF-induced redistribution of uPAR. (*D*) HUVECs pre-treated with wortmannin (0.1 μM; PI3-kinase inhibitor) or MMP2/9 inhibitor (1 μM) were stimulated with either VEGF-E or PIGF. (50 ng/mL, each). The surface levels of β1-integrins were determined by flow cytometry as in Figure 1B.

Europe PMC Funders Author Manuscripts

Europe PMC Funders Author Manuscripts

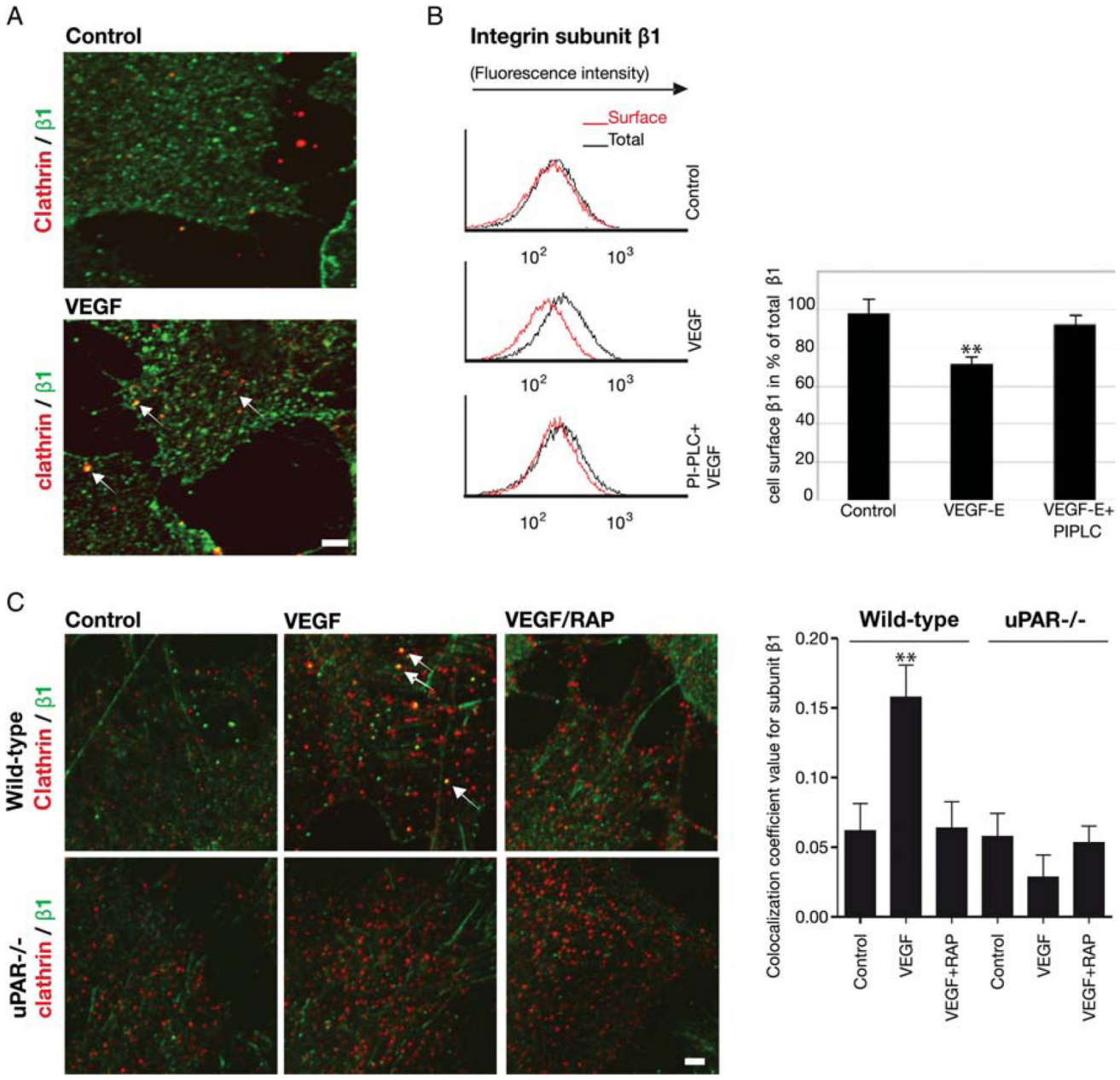

Figure 3.

VEGF-induced internalization of β1-integrins is contingent on uPAR. (*A*) Confocal images of fixed and permeabilized control and $VEGF_{165}$-stimulated (50 ng/mL, 30 min) HUVECs immunostained for clathrin heavy chain (green) and β1-integrins (red) to visualize their co-localization (*arrows*). (*B*) Removal of uPAR from the endothelial cell surface by treatment with PI-PLC diminishes VEGF-induced internalization of β1-integrin. HUVECs were treated with 5 U/mL of PI-PLC for 15 min and stimulated with VEGF-E (50 ng/mL) for 60 min. Cell surface levels of β1-integrins were determined as in Figure 1B; ($n = 3$), mean ± standard deviation, $^{**}P < 0.01$ vs. control, *t*-test for paired data. (*C*) VEGF-induced co-localization of β1-integrins and clathrin is absent in $uPAR^{-/-}$ murine endothelium.

Endothelial cells isolated from the pulmonary microvasculature were pre-incubated in the absence and presence of RAP (200 nM) for 15 min, stimulated with murine $VEGF_{164}$ (50 ng/mL), fixed and permeablized. Immunostaining for clathrin heavy chain (green) and β1-integrins (red) was visualized by confocal microscopy and their co-localization (*arrows*) quantified by the ImageJ software, which is summarized in the bar diagram; mean ± standard deviation ($n = 8$). $^{**}P < 0.05$ (ANOVA). Scale bar = 6 μm.

Europe PMC Funders Author Manuscripts

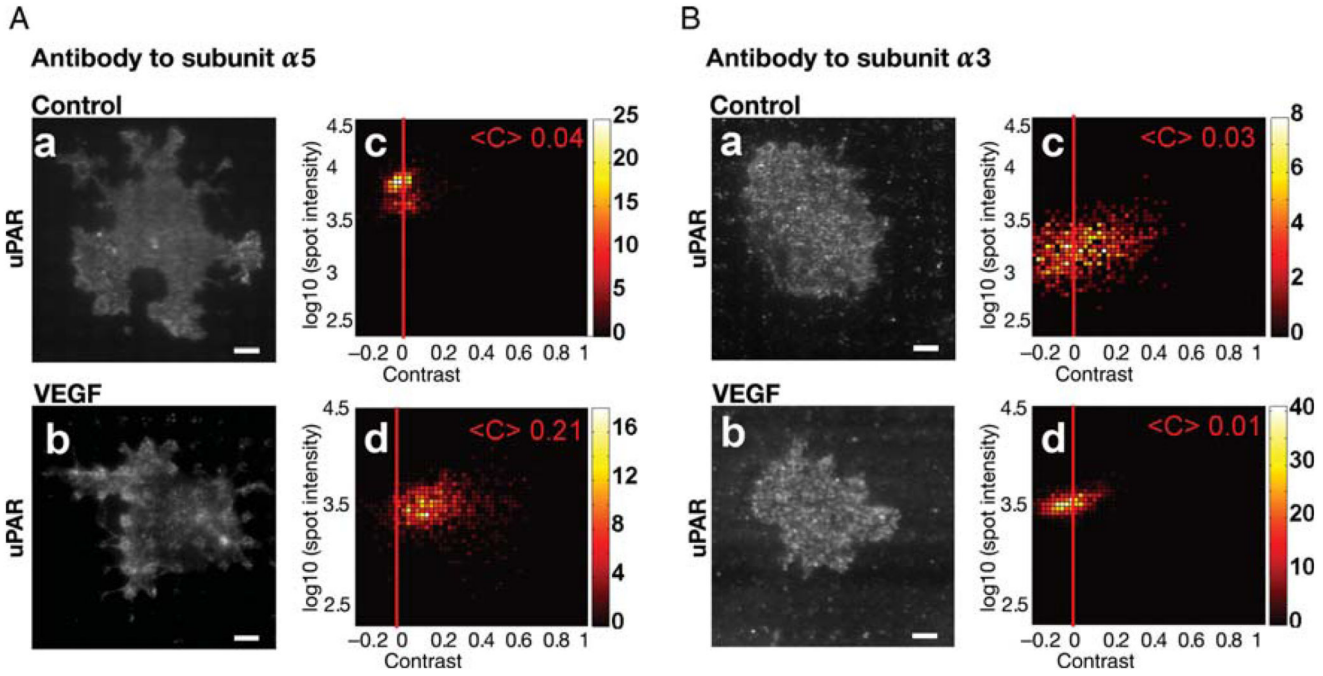

Figure 4.

VEGF-induced interaction of uPAR with the fibronectin receptor integrin-α5β1. HUVECs were grown on microchips patterned with antibodies against α5- (*A*) or α3-integrins (*B*). After stimulation with $VEGF_{165}$ (50 ng/mL) for 60 min, cells were fixed and immunostained with a fluorescent monoclonal antibody against uPAR. Representative TIRF images visualize $VEGF_{165}$-induced uPAR redistribution to mimic the pattern of the antibody to integrin subunit α5 (cf. A.a and A.b), which is absent on surfaces coated with an antibody to integrin subunit α3 (cf. B.a and B.b); scale bar = 6 μm. Colour density plots (A.c, A.d; B.c, B.d) summarize the data from 100 to 120 cells.

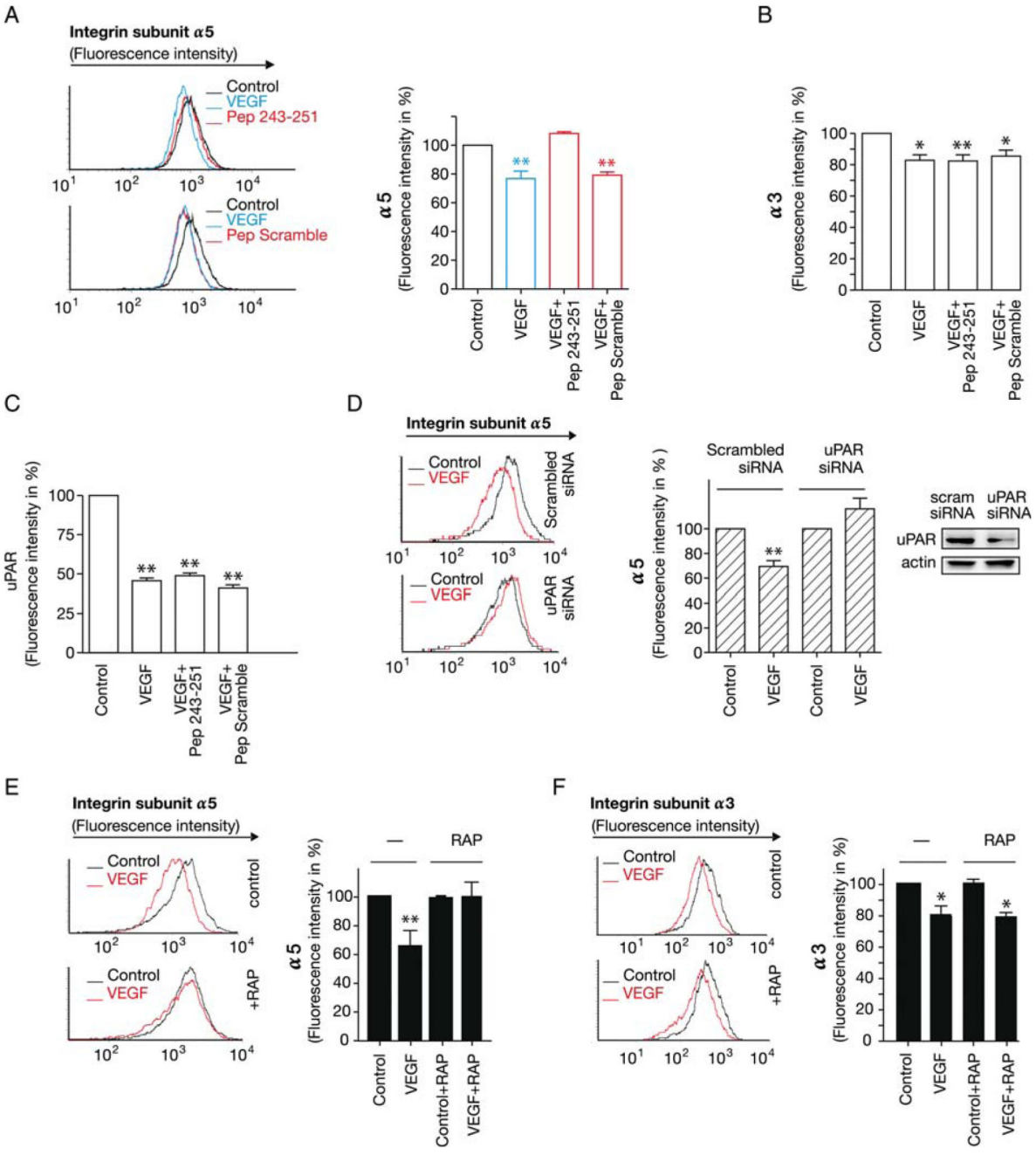

Figure 5.

VEGF-induced internalization of integrin-α5β1 requires uPAR. Inhibition of VEGF-induced internalization of integrin-α5β1 (*A*) but not of integrin-α3β1 (*B*) or of uPAR (*C*) by Pep 243–251, a peptide derived from human uPAR. HUVECs were pre-treated with Pep 243–251 (25 μM) or the scrambled control peptide (Pep scramble, 25 μM) for 10 min and stimulated with $VEGF_{165}$ (50 ng/mL) for 60 min. Cell surface expression of integrin-α5β1 (*A*), integrin-α3β1 (*B*) or of uPAR (*C*) was quantified by flow cytometry. Bar diagram summarizes four experiments (mean ± standard deviation) with immunostaining in control

cells representing 100%. (*D*) Knock-down of uPAR by siRNA impairs VEGF-induced internalization of integrin-α5β1 assessed by flow cytometry. Immunoblotting for uPAR and actin (loading control) in lysates of siRNA-trasfected cells. (*E* and *F*) RAP inhibits VEGF-induced internalization of integrin-α5β1 but not of -α3β1. Endothelial cells were treated with RAP (200 nM) for 30 min prior to stimulation with VEGF for 60 min; bar diagrams summarize data from three flow cytometry experiments (mean ± standard deviation) (** $P < 0.01$).

Europe PMC Funders Author Manuscripts

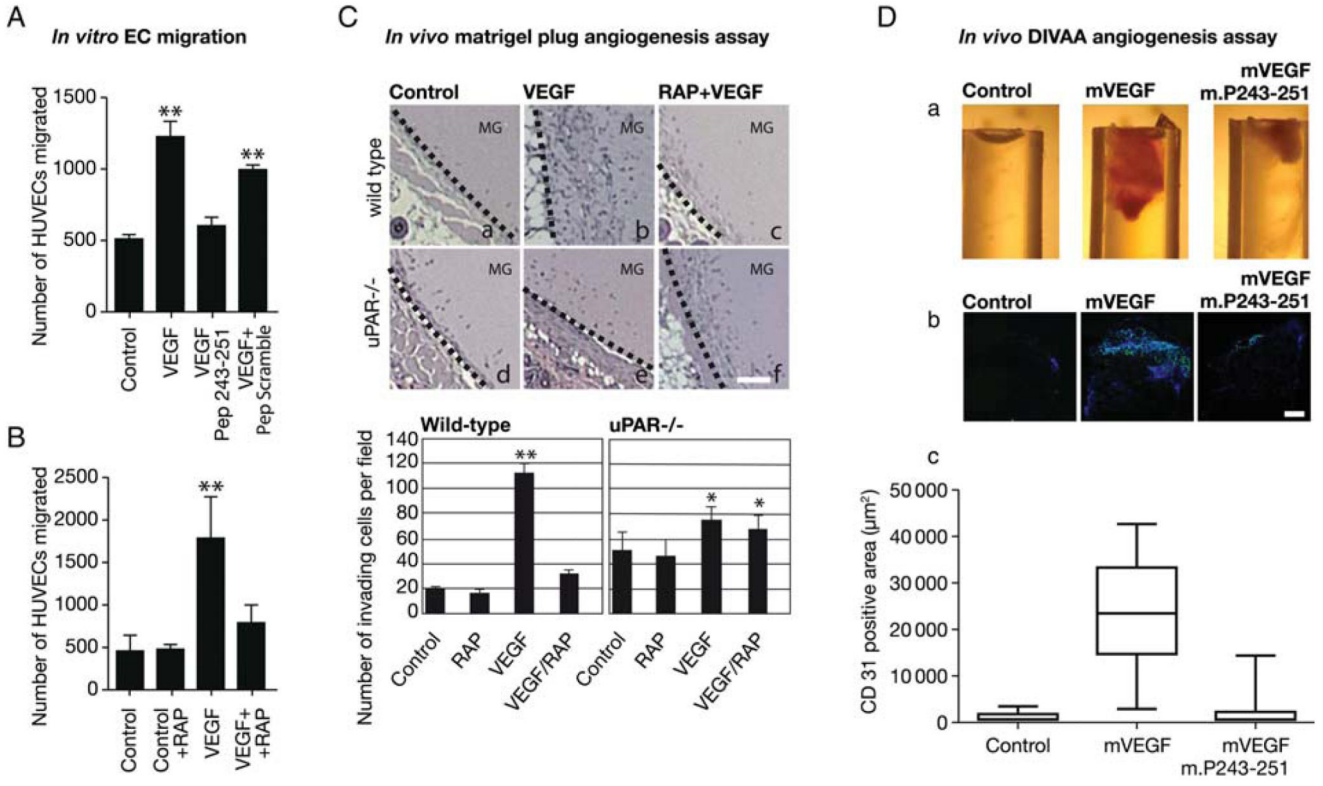

Figure 6.

VEGF-induced endothelial migration *in vitro* (*A* and *B*) and *in vivo* (*C* and *D*) requires the interaction of the fibronectin receptor integrin-α5β1 with uPAR. Serum-starved HUVECs were treated with the uPAR-derived (Pep 243–251, 25 μM) or the control peptide (PScramble, 25 μM) (*A*) or with RAP (200 nM) (*B*) for 10 min and then allowed to migrate through Transwell membranes towards $VEGF_{165}$ for 4 h at 37°C. Cells that had migrated to the underside of the membrane were fixed and counted (AnalySiS® software, Olympus). The results from three (*A*) and four (*B*) independent experiments are shown; statistically significant differences were verified by ANOVA (**$P < 0.01$). (*C*) Matrigel plug *in vivo* angiogenesis assay: control matrigel or matrigel containing murine $VEGF_{164}$ (300 ng/mL) or the combination of $VEGF_{164}$ and RAP (200 nM) was injected subcutaneously into wild-type and uPAR-deficient animals. Representative images show haematoxylin-stained sections that include the plug and surrounding tissue (dotted line indicates border) (scale bar = 200 μm). Bar graphs show the quantification of plug-invading cells for 8 plugs/condition. (*D*) Impaired angiogenesis in the presence of uPAR-derived peptide. For the directed *in vivo* angiogenesis assay, angioreactors of 1.0 cm length and 0.15 cm diameter were filled with basement membrane extract either alone or containing 2 μg/mL $VEGF_{164}$ and 1 mg/mL heparin with or without the peptide m.P243-251 (TASWCQGSH) derived from murine uPAR (250 μM). A reactor was implanted subcutaneously into either flank of 6–8-week-old BL6 mice for 11 days. (a) Representative explanted reactors showing macroscopically discernible VEGF-induced invasion of the matrigel-filled reactors (b) Representative micrographs of sections stained with rat anti-mouse CD31 antibody and Hoechst, photographed and analysed using the CellP® imaging software (Olympus); size bar 100 μm.

(c) Quantification of invading endothelial cells (CD31positive, green); box plots show the median and the 25–75% quartile and whiskers indicate the 95% confidence interval ($n = 8$); the difference between mVEGF and the other conditions was statistically significant ($P < 0.05$; ANOVA).

Europe PMC Funders Author Manuscripts